EXPERIMENTAL STUDIES OF HIGH-SPEED LIQUID FILMS ON DOWNWARD-FACING SURFACES FOR IFE WET WALL CONCEPTS

J. K. Anderson, S. G. Durbin, D. L. Sadowski, M. Yoda[†], S. I. Abdel-Khalik

and the ARIES Team

G. W. Woodruff School of Mechanical Engineering

Georgia Institute of Technology

Atlanta, GA 30332-0405 USA

Number of pages: 15

Number of figures: 8

Number of tables: 0

[†] Corresponding Author:

Minami Yoda
School of Mechanical Engineering
771 Ferst Dr.
Atlanta, GA 30332-0405 USA

E-mail: minami.yoda@me.gatech.edu
Phone: (404) 894-6838
Fax: (404) 894-8496

EXPERIMENTAL STUDIES OF HIGH-SPEED LIQUID FILMS ON DOWNWARD-FACING SURFACES FOR IFE WET WALL CONCEPTS

J. K. Anderson, S. G. Durbin, D. L. Sadowski, M. Yoda, S. I. Abdel-Khalik
and the ARIES Team

ABSTRACT

The fusion event in inertial fusion energy (IFE) reactors creates neutrons, photons and charged particles that can damage the chamber first walls. The Prometheus design study used a high-speed thin film of molten lead injected tangential to the wall to protect the upper endcap of the reactor chamber from damaging x-rays and target debris (1,2). To assure full chamber coverage, the film must remain attached. Film detachment under the influence of gravity is most likely to occur on the downward facing surfaces over the upper endcap of the reactor chamber. Accurate numerical predictions of detachment length are effectively impossible in this turbulent flow due to difficulties in determining appropriate boundary conditions near the detachment point.

As part of the ARIES-IFE study, experimental investigations of high-speed water films injected onto downward-facing planar surfaces at angles of inclination up to 45° below the horizontal were therefore performed. The initial growth and subsequent detachment of films with initial thickness up to 2 mm and injection speeds up to 11 m/s were measured. To our knowledge, these experiments are the first to investigate the detachment of turbulent liquid films on downward facing surfaces. The implications of these initial results on thin liquid protection and the "wet wall" concept are discussed.

I. INTRODUCTION

A number of inertial fusion energy (IFE) power plant design studies have considered using a sacrificial layer to protect the first wall. In thin liquid protection, a sacrificial liquid film flowing along the reactor chamber walls absorbs essentially all the x-rays and charged particles from the fusion event, protecting the first wall from damaging radiation and thermal stresses. The Prometheus study (1,2), which considered thin liquid protection for both heavy-ion beam and laser ignition reactors, proposed using a film of liquid lead to protect the silicon carbide first walls of the reactor chamber, a vertical cylinder with hemispherical upper and lower endcaps with a radius of curvature of 5 m. The film was created using two different systems: 1) a "wetted wall" with a 0.5 mm thick layer of liquid lead supplied through a porous SiC structure; and 2) a "wet wall" with a "film injector" injecting liquid lead through slots at the top of the chamber to create a film a few millimeters thick in contact with the first wall over the upper chamber endcap. The sacrificial lead layer was vaporized by each fusion microexplosion, requiring re-condensation and re-establishment of a fresh layer before the next microexplosion.

Both the wetted and wet wall concepts are currently under investigation as part of the ARIES-IFE study (3). The work described here focuses on the basic hydrodynamics of the wet wall concept. There are several major design issues for robust and effective protection of the upper endcap of the reactor chamber using the wet wall concept. The most important design issue is prevention of the formation of "dry patches" on the first wall, or patches with no protective liquid layer. Consider dry patch formation in a film flow driven by forces tangential to the surface (*e.g.*, thermocapillary and surface forces). Recent results using minimum total energy criteria show that, for an isothermal liquid

film flowing down a vertical adiabatic wall (4), the minimum film thickness required to re-wet any dry patch is less than 1 mm for most IFE coolants of interest with contact angles ranging from 0° to 90° (5). Moreover, the minimum film speed (based upon minimum wetting rate) required for a stable fully wetted liquid film is less than 1 m/s under the same conditions. The minimum required film thickness is proportional to the square of the gravitational acceleration component along the flow direction. (4). The minimum required film speed, on the other hand, is weakly dependent on gravity ($\sim g^{-0.2}$, where g is gravitational acceleration) and strongly dependent on surface tension ($\sim\sigma^3$, where σ is the surface tension). Hence, at the expected liquid film velocities in IFE systems (which are much greater than 1 m/s), dry patch formation in a film flowing over a vertical wall is the "worst case" from a purely hydrodynamic viewpoint, since the streamwise component of gravity is greatest for this orientation.

In the absence of dry patches, preventing detachment of the film from the first wall—which would partially uncover the surface, thereby negating its effectiveness as a wall protectant—is then the most important design issue, inasmuch as it will dictate the spacing of liquid injection and extraction points on the cavity surface. If the curvature of the first wall is negligible, a reasonable assumption given that the radius of curvature for the Prometheus chamber upper endcap is 5 m, or at least three orders of magnitude greater than the film thicknesses of $O(10^{-3}$ m) and film radii of curvature at the detachment point of $O(10^{-2}$ m), the appropriate model problem is a film flowing over a flat surface at various angles of inclination with respect to the horizontal. Detachment is most likely to occur on films flowing over downward-facing surfaces (*i.e.*, surfaces at a negative angle of inclination with respect to the horizontal), where the component of gravity normal to the surface promotes film detachment. Moreover, this flow

geometry—where a denser "heavy" liquid flows above a less dense "light" near-vacuum—may be susceptible to droplet and even dry patch formation due to Rayleigh-Taylor instability.

As the first part of our study of the wet wall concept, turbulent films on downward-facing surfaces were therefore experimentally studied by injecting water through rectangular slot nozzles tangentially onto the underside of a glass plate in atmospheric pressure air. The effect of initial film (*i.e.*, nozzle) thickness δ, initial film injection velocity U and plate inclination angle below the horizontal θ was characterized in terms of the Froude, Reynolds and Weber numbers, or $Fr = U/\sqrt{g(\sin\theta)\delta}$, $Re = U\delta/\nu$ and $We = \rho U^2\delta/\sigma$, respectively. Here, g is the gravitational acceleration, ν is the fluid kinematic viscosity, and σ is the surface tension between the fluid and the surrounding gas. In these initial studies, δ = 1–2 mm, U = 1.9–11 m/s, and θ = 0–45°, giving Fr = 15–121, Re= 3700–21000 and We = 100–3200.

To our knowledge, there have been few studies of turbulent liquid films on downward-facing surfaces. Hashidate *et al.* (6) studied films on a downward-facing acrylic surface for Re = 10–500 and θ = 0–30° for water with surfactants to vary the surface tension, and concluded that surface roughness had a major impact on detachment length. These results on film detachment and lateral spread—the first to our knowledge for such high Reynolds number turbulent liquid films—will help provide an experimental design database for wet wall concepts in thin liquid protection of IFE reactor chamber first walls.

II. EXPERIMENTAL APPARATUS AND PROCEDURES

A. Flow Loop

The pump-driven recirculating flow loop used to produce the thin liquid films is shown in Figure 1. Water is driven by a 0.5 hp centrifugal pump (Teel 2P39C) through an adjustable butterfly valve and a flexible coupling (A). The water passes through a flow straightening section (B) and exits through a rectangular nozzle (C) at an adjustable angle with respect to the horizontal. The water is injected by the nozzle tangentially onto the underside of a tempered float glass plate of width 0.4 m extending a distance x = 0–183 cm downstream of the nozzle exit. The flow, which either detaches from the glass surface or hits a vertical splash guard at the downstream end of the glass plate, then falls into a 840 L (220 gal) receiving tank below, where it is recirculated by the pump. The coordinate system for this flow is defined as follows: x along the flow direction, y along the long dimension of the film or parallel to the glass surface, and z downwards along the short dimension of the film or normal to the glass surface.

Three different nozzles, all fabricated using stereolithography rapid prototyping at the Georgia Tech Rapid Prototyping and Manufacturing Institute from DSM Somos® 7110 resin, were used in these experiments. The fabrication tolerance was 0.1 mm, based upon the spatial resolution of the rapid prototyping machines. All the nozzles have a two-dimensional 5^{th} order polynomial contraction in their z-dimension from 1.5 cm upstream to δ over an x-extent of 2 cm, followed by a straight channel with an x-extent of 1 cm (Fig. 2). This type of contraction is extensively used in wind tunnels and water channels to produce uniform flow with thin boundary layers. The nozzles have a y-dimension at their exit of 5 cm, giving rectangular exits with aspect ratios of 50, 33, and

25 for nominal initial film thicknesses at the nozzle exit of δ = 1, 1.5 and 2 mm, respectively. In all experiments, the water was injected parallel to the glass plate by clamping the nozzle along its entire *y*-extent at its straight channel exit section parallel to and flush with the underside of the glass plate using two parallel Plexiglass plates.

The flow straightening section, also fabricated from DSM Somos® 7110 resin, consisted of a perforated plate (53.6% open area ratio, 0.21 cm diameter staggered holes), followed by a 1.8 cm section of honeycomb with cell diameter 0.16 cm, both of stainless steel. The edge-to-edge spacing between the perforated plate and honeycomb and the honeycomb and the nozzle inlet was 7 mm and 50 mm, respectively. The butterfly valve adjusts the flow rate and hence initial film velocity U at the nozzle exit. In all cases, U is determined using a Rotameter-type flowmeter just upstream of the butterfly valve (*cf.* Fig. 1).

B. Flow Visualization

The film first spreads laterally (*i.e.*, along the surface of the glass plate), then detaches from the glass plate some distance downstream of the nozzle exit. This film "detachment length" x_d and the lateral dimension, or width, of the film W were studied as a function of various flow parameters. Although droplet formation was typically observed at the film free surface upstream of the detachment point, no dry patch formation was observed before detachment. Detachment length x_d was measured by imaging the turbulent water films from the side to obtain x–z planes ("side views") of the flow, which was illuminated obliquely from below (*cf.* Fig. 1) by a 425W lamp. Individual images were recorded at an exposure of 8 ms by a progressive scan CCD camera (Pulnix TM-9701) onto the RAM of a PC using a framegrabber card

(ImageNation PX610A) as 8-bit grayscale 640 col × 480 row images. Each individual image spans 7τ–90τ, where the flow convective time scale $\tau = \delta / U = 0.09 - 1.1$ ms. A ruler attached to the upper side of the glass plate was used to measure the detachment length x_d (in inches), defined here as the distance measured along x from the nozzle exit where the film detaches from the plate surface (Fig. 3*a*) on each image. The film detaches at slightly different x-locations across the lateral (y) extent of the film at low U and the largest value of δ = 2 mm (Fig. 3*b*). In all cases, the detachment distance on each image was therefore taken to be the smallest x value, or the location farthest upstream, at which film detachment occurred. Since the detachment distance on a single image can vary by up to ±3.5 cm for this turbulent flow, the values reported here for x_d are the average of 20 independent realizations obtained from images taken of the flow over about 60 s.

The film width, or y-extent, $W(x)$ was measured through the top of the glass plate as a function of distance downstream of the nozzle by direct visual inspection (Fig. 4), with data obtained every 5 cm for $x < x_d$. In all the experimental cases studied here, $W(x)$ varied by less than ±1 mm over time at any given downstream location. Initially, the film spreads along and normal to the glass surface after leaving the nozzle, with lateral (*i.e.*, along the y-direction) spreading rates dW/dx much greater than those normal to the surface, or along the z-direction. The lateral spreading rate then decreases, with W (*vs.* dW/dx) decreasing at lower Fr, before gravitational effects overcome surface tension effects and the film detaches from the underside of the glass plate.

III. RESULTS AND DISCUSSION

A. Detachment Distance x_d

The average detachment distance normalized by initial film thickness x_d/δ is shown as a function of *Fr* for δ = 1 mm (open symbols), 1.5 mm (black symbols) and 2 mm (gray symbols); and $\theta = 0°$ (squares), 10° (diamonds), 30° (triangles) and 45° (circles) in Figure 5. In the cases where gravitational effects normal to the plate are weakest (large θ, small δ, and large *Fr*), film detachment was not observed over the entire glass plate, implying that $x_d > 183$ cm; obviously no data are presented for these cases. In the cases where detachment was observed, the nondimensional detachment distance increases with *Fr*, as expected, since gravitational effects normal to the plate become smaller as *Fr* increases. Although the actual value of x_d/δ varies with both δ and θ, the slope of the various x_d/δ curves for each δ and θ appears to be similar, suggesting that the growth rate of nondimensional detachment length with *Fr* is independent of initial film thickness and inclination angle. A "virtual origin", such as those used in various types of turbulent flows may then be used to account for different initial conditions between various experimental runs. There also appears to be a slight "leveling off" of the x_d/δ curves at higher *Fr* (*cf.* open triangles and diamonds, for example). These detachment distance data were also plotted as functions of *Re* and *We*, but no clear trends were observed. The Froude number therefore appears to be the only significant dimensionless group for characterizing detachment distance. This result is hardly surprising, since *Fr* is the only one of these three dimensionless groups that includes the effects of gravity and plate inclination angle, parameters which both have a significant impact on film detachment.

In the Prometheus design, δ = 0.5 mm and $U > 8$ m/s, giving $Fr > 120$. Extrapolation of the detachment length data in Figure 5 suggest that a film injected at the

top of the endcap ($\theta \approx 0^o$) will have a mean detachment length $x_d > 1600\delta = 0.8$ m. Given that the hemispherical upper endcap of radius 5 m will have a dimension along its co-latitude of 7.9 m from top to bottom, the protective film will detach and form droplets well before the end of the endcap. Maintaining an attached film over the entire upper endcap will therefore require some type of "composite" structure, possibly involving several injection slots over the co-latitude of the endcap and some type of suction downstream of each injection slot to remove the film before it detaches.

We hypothesize that the major sources of error in these data are slight misalignments between the nozzle and the glass plate and variations in the initial film thickness δ due to our fabrication tolerances. The maximum misalignment between the y-axis of the nozzle and the surface of the glass plate is about 1^o, resulting in a height difference of 0.9 mm, or $0.45–0.9\delta$, across the 5 cm y-extent of the nozzle exit. The minimum geometric tolerance for these nozzles, based upon the spatial resolution of the rapid prototyping machine used to fabricate these components, is 0.1 mm absolute, or 5–10% of δ. The resultant variation in initial film thickness over the y-extent of the nozzle with respect to the glass surface due to these two factors can affect detachment distance and film width by introducing local variations in pressure gradient and flow speeds.

Other potential sources of error in these data include local variations in the wettability of the glass plate due to surface and liquid contamination. The contact angle of water on the glass plate used in these experiments was estimated by visual inspection to lie between 30° and 35°. Although the glass plate was cleaned with a commercial ammonia-based glass cleaner at the beginning of each experimental run, the contact angle varies over the glass surface by at least a few degrees due to contamination of the water (which remained in the facility for up to a week) and the glass plate. Nevertheless, little

variation was observed in either mean detachment length or film width over independent experimental runs under otherwise identical conditions. The geometry of the glass plate is not considered to be a significant source of error in these experiments, since the overall curvature of tempered glass should be minimal, and the average surface roughness of glass manufactured using the float process is typically less than 10^{-6} m.

The trends observed in Figure 5 are most consistent for $\delta = 2$ mm (gray symbols), where variations in initial film thickness due to nozzle-plate misalignment and nozzle fabrication tolerances are the smallest for the cases studied. Data obtained for the $\delta = 2$ mm nozzle were therefore used to characterize the lateral spreading rate of the film, as discussed in the next subsection.

B. Average Film Width *W*

Figure 6 shows the film width or *y*-extent along the glass surface normalized by the exit width W/W_o as a function of distance downstream of the nozzle exit normalized by the initial film thickness x/δ for $\delta = 2$ mm and $Re = 18000$ at $\theta = 0°$ (squares), 10° (diamonds), 30° (triangles) and 45° (circles). The initial width of the film at the nozzle exit $W_o = 5$ cm in all cases. For $x/\delta \leq 400$, the film width is essentially independent of θ, probably because the effects of initial conditions are dominant in this "near-field" region of the flow, and the film spreads until it is more than 3.5 times its initial width. In the "far-field" region ($x/\delta > 400$), however, dW/dx increases with θ. The film width actually decreases for $\theta = 0°$ and 10°, suggesting that the film must have significant growth normal to the plate to conserve linear momentum. At higher angles of inclination, namely $\theta = 30°$ and 45°, the sheet continues to grow in the far-field region, reaching widths nearly quintuple its initial value. The marked lateral growth observed for these

films is in agreement with previous experimental results for three-dimensional turbulent wall jets, where fluid is injected through a rectangular slot into a large quiescent reservoir of the same fluid. Recent simulations show that the remarkable lateral spread of these flows is primarily due to the creation of streamwise vorticity (7). The W/W_o curves for both angles are essentially the same, suggesting that the film reaches an asymptotic shape (at least in y-dimension) at higher values of inclination angle. Finally, the film does not separate until $x/\delta > 400$ in all cases.

Figure 7 shows dimensionless film width W/W_o plotted as a function of normalized downstream distance x/δ at $\delta = 2$ mm and $\theta = 30°$ for $Re = 7500$ ($\times$), 12400 (∇) and 18600 (+). Here, W is independent of Re (*vs.* θ in Fig. 6) for $x/\delta \leq 400$. The film width also appears to be independent of Re at the two higher Re, suggesting that the film reaches an asymptotic shape (at least along the y-direction) above a certain Re.

Defining the streamwise extent of the near-field region as x_c, and the mean width of the film at the end of the near-field region as W_c (*i.e.*, $W(x_c) = W_c$), Figure 8 shows a graph of W_c / W_o as a function of Fr for all experimental cases studied here: $\delta = 1$ mm (open symbols), 1.5 mm (black symbols) and 2 mm (gray symbols); and $\theta = 0°$ (squares), 10° (diamonds), 30° (triangles) and 45° (circles). For Froude numbers above about 40, W_c, which is an indication of the maximum y-dimension of the flow, is essentially independent of Fr and δ. W_c appears to increase slightly with θ, however, with $W_c / W_o \approx 3.6 - 4.5$ for $\theta = 0°$–45°. Although not shown here, similar trends were observed for W_c / W_o as a function of Re. The marked lateral spread of these film flows suggest that the longitudinal spacing of injection slots in the Prometheus design can be 3–4 times their longitudinal dimension while still maintaining adequate coverage, assuming

that adjacent films merge smoothly.

IV. SUMMARY

Mean detachment distance and average film width (*i.e.*, dimension along the plate) were experimentally characterized for thin turbulent liquid films on downward-facing surfaces for various flowrates, initial film thicknesses and angle of inclination. In many cases, droplet formation was observed at the film free surface upstream of the detachment point. In all cases, dry patch formation was not observed. Although the absolute value of detachment distance is determined by the initial flow conditions, change in mean detachment distance was found to be a function only of Froude number, a dimensionless group characterizing the relative importance of inertial and gravitational effects. The flow has a large lateral spread along the surface, growing up to fivefold in the *y*-dimension. Based upon this lateral growth, we define a "near-field" region of the turbulent film where the lateral growth is determined by initial conditions and appears independent of other flow parameters such as Reynolds number. The lateral dimension of the flow at the end of this region appears to be essentially independent of Froude number and initial film thickness, but appears to depend weakly upon inclination angle. The lateral growth of the flow in the "far-field" region farther downstream is a strong function of inclination angle, with the film lateral dimension actually decreasing at small angles of inclination. In all cases, the film detaches in the far-field.

In terms of implications for the wet wall concept, the initial results from this experimental study of turbulent liquid films flowing over downward-facing surfaces suggest:

1) Any film injected at the top of the upper endcap of the reactor chamber in the Prometheus design will detach well before the bottom of the endcap. At a minimum, the wet wall concept will therefore require multiple injection slots and some mechanism to remove liquid before the film forms droplets or detaches.
2) The injected films will spread to at least 3.5 times their initial width, improving the lateral (presumably longitudinal) spacing requirements for the injection slots.

The aim of this study is to provide "design windows" for thin liquid protection schemes. Given that the Prometheus study reported that liquid lead did not wet silicon carbide, and suggested that this issue required further consideration, we intend next to characterize the effect of wettability or contact angle on film detachment and lateral spread by studying turbulent films of water on downward-facing surfaces of various chemical composition (*e.g.*, Teflon). Studies of how turbulent liquid film flows recover around cylindrical dams representing penetrations into the chamber first wall for target injection and ignition beam propagation are also planned. Since this flow is likely to separate around the dam and possibly form droplets, then "reattach" some distance downstream of the trailing edge of the dam (much like uniform flow around a circular cylinder), some type of aerodynamic fairing may be required on the downstream end of the penetrations to protect the first wall in the neighborhood of a beam or target injection port.

ACKNOWLEDGMENTS

This work was performed as part of the ARIES-IFE study supported by the U.S. Department of Energy Office of Fusion Energy Sciences through contract #DE-FG02-

01ER54656. We thank the members of the ARIES project team for numerous discussions and helpful suggestions.

REFERENCES

[1] L. M. Waganer *et al.* (1992) *Inertial Fusion Energy Reactor Design Studies: Prometheus Final Report*. MDC 92E0008 (DOE/ER-54101).

[2] L. M. Waganer, "Innovation leads the way to attractive inertial fusion energy reactors—Prometheus-L and Prometheus-H," *Fusion Engineering and Design*, **25**, 125 (1994).

[3] S. Shin, F. Abdelall, D. Juric, S. I. Abdel-Khalik, M. Yoda, D. Sadowski, and the ARIES team, "Fluid dynamic aspects of the porous wetted wall protection scheme for IFE reactors," submitted to *Fusion Science and Technology* (2002).

[4] M. S. El-Genk and H. H. Saber, "Minimum thickness of a flowing down liquid film on a vertical surface," *International Journal of Heat and Mass Transfer*, **44**, 2809 (2001).

[5] S. I. Abdel-Khalik and M. Yoda, "Design considerations for thin liquid film wall protection scheme," ARIES Project E-Meeting Presentation, (October 24), http://aries.ucsd.edu/ARIES/MEETINGS/0110/ (2001).

[6] Y. Hashidate, K. Shioda and S. Nonaka, "Experimental study on the flow behavior of a liquid film on an inclined downward-facing plate," *Transactions of the Japan Society of Mechanical Engineers B*, **59**, 770 (1993) [Japanese with English abstract].

[7] T. J. Craft and B. E. Launder, "On the spreading mechanism of the three-dimensional turbulent wall jet," *Journal of Fluid Mechanics*, **435**, 305 (2001).

FIGURE CAPTIONS

Figure 1 Schematic of flow loop (side view).

Figure 2 Nozzle cross-section.

Figure 3 Typical side view images near the film detachment point showing an x–z plane of the flow and the detachment distance x_d for $\delta = 0.1$ cm, $\theta = 10°$, $Fr = 90$, $Re = 8600$, $We = 1070$ (*a*) and for $\delta = 0.2$ cm, $\theta = 0°$, $Fr = 13.5$, $Re = 3600$, $We = 98$ (*b*). Note the detachment of the water from the glass plate on the lower right side of both images, and the multiple detachment points in (*b*). The ruler on the top of both images is in inches.

Figure 4 Image of the turbulent film viewed at an obliqud angle through the glass plate for $\delta = 0.1$ cm, $\theta = 30°$, $Fr = 81$, $Re = 7200$, $We = 790$. Here, the sheet width $W(x)$ increases from about 7.5 cm to 18 cm over an downstream extent of 23 cm. Although not evident in this view, the film is essentially symmetric around its centerline (the x-axis).

Figure 5 Plot of nondimensional detachment distance x_d/δ vs. Froude number Fr for $\delta =$ 1 mm (open symbols), 1.5 mm (black) and 2 mm (gray) and $\theta = 0°$ (squares), 10° (diamonds), 30° (triangles) and 45° (circles).

Figure 6 Plot of normalized average film width as a function of the ratio of distance downstream of the nozzle exit to initial film thickness for $\theta = 0°$ (squares), 10° (diamonds), 30° (triangles) and 45° (circles) for $\delta = 2$ mm, $Re = 18000$, $We = 2450$.

Figure 7 Normalized average film width *vs.* normalized downstream distance at δ = 2 mm, $\theta = 30°$ for Re = 7500 ($\times$), 12400 (∇) and 18600 (+).

Figure 8 Plot of normalized film width at the end of the near-field region W_c/W_o as a function of Froude number Fr for δ = 1 mm (open symbols), 1.5 mm (black) and 2 mm (gray) and $\theta = 0°$ (squares), 10° (diamonds), 30° (triangles) and 45° (circles).

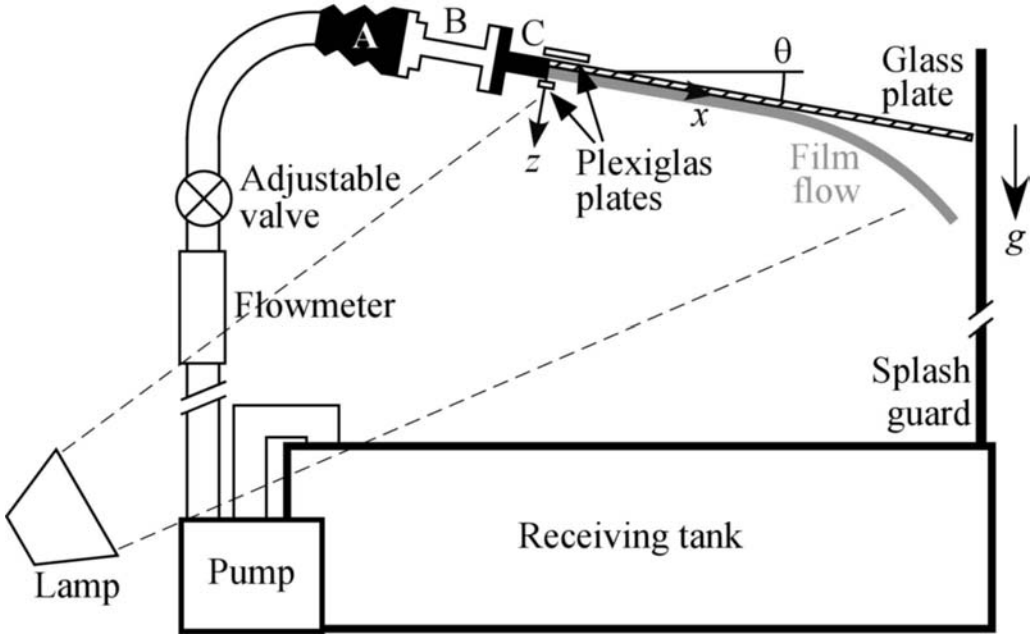

Figure 1

Anderson *et al.*

Ms-272402

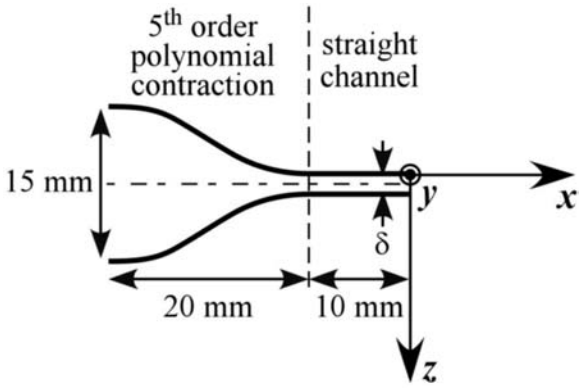

Figure 2

Anderson *et al.*

Ms-272402

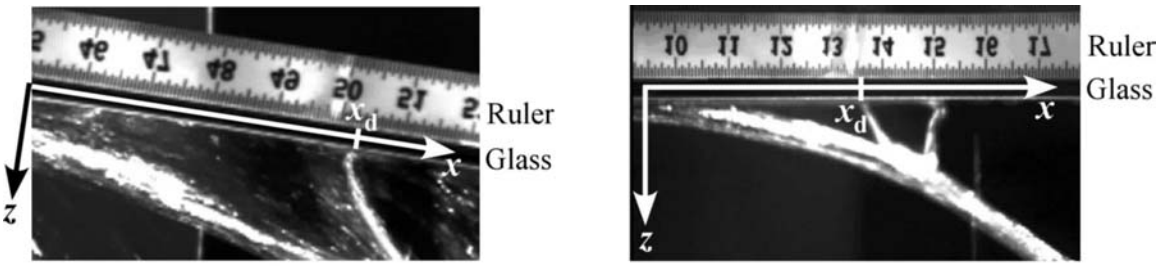

Figure 3

Anderson *et al.*

Ms-272402

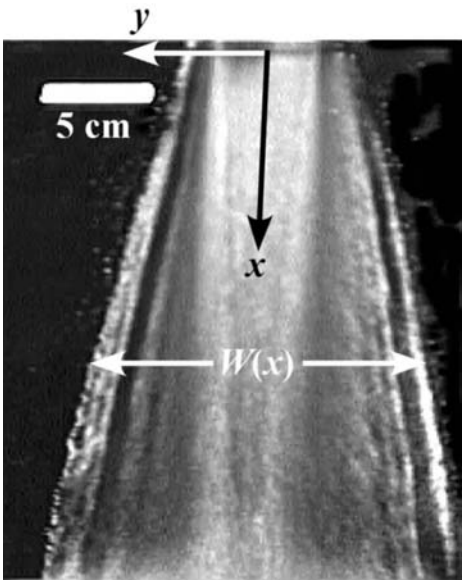

Figure 4

Anderson *et al.*

Ms-272402

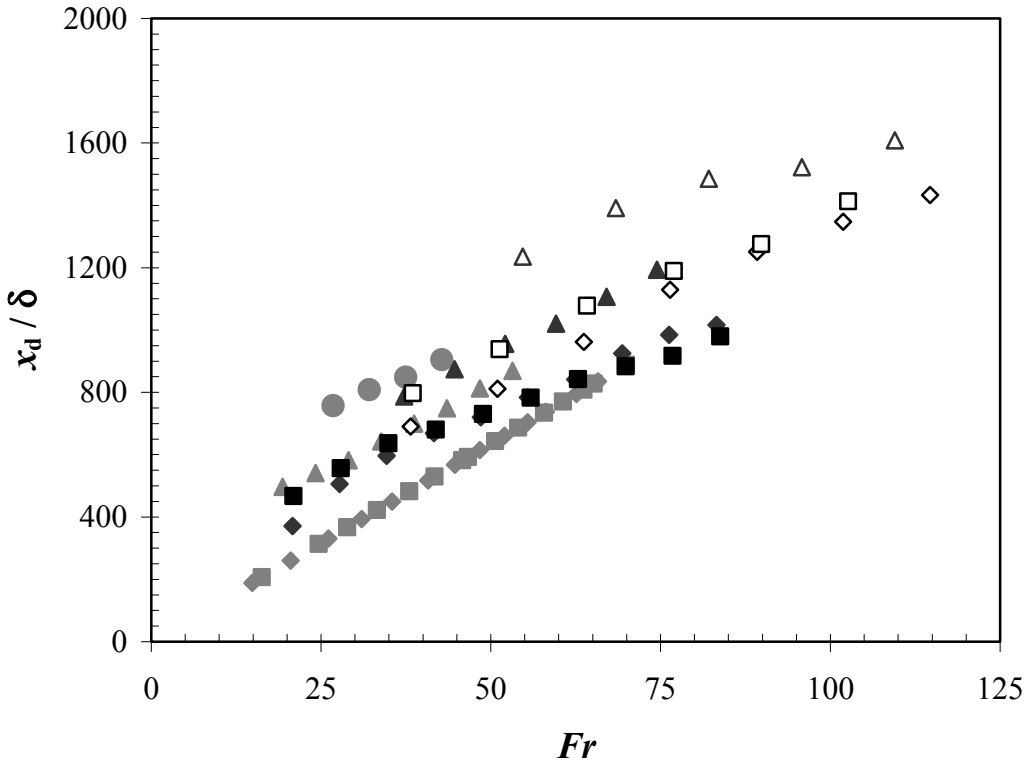

Figure 5

Anderson *et al.*

Ms-272402

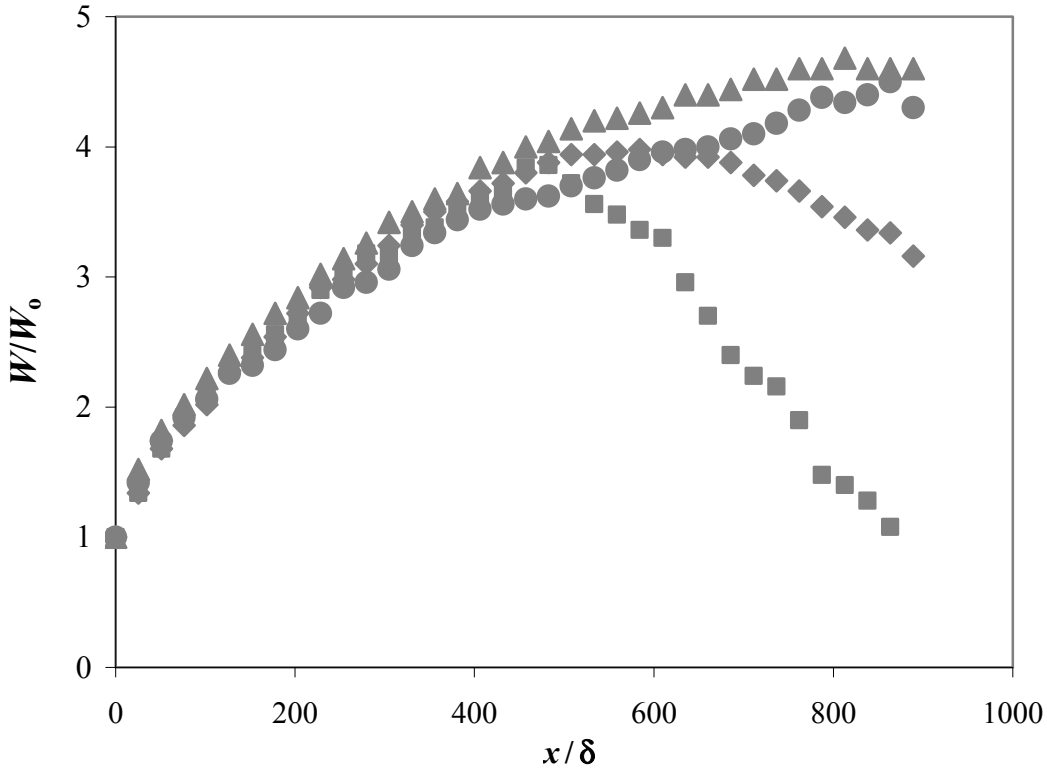

Figure 6

Anderson *et al.*

Ms-272402

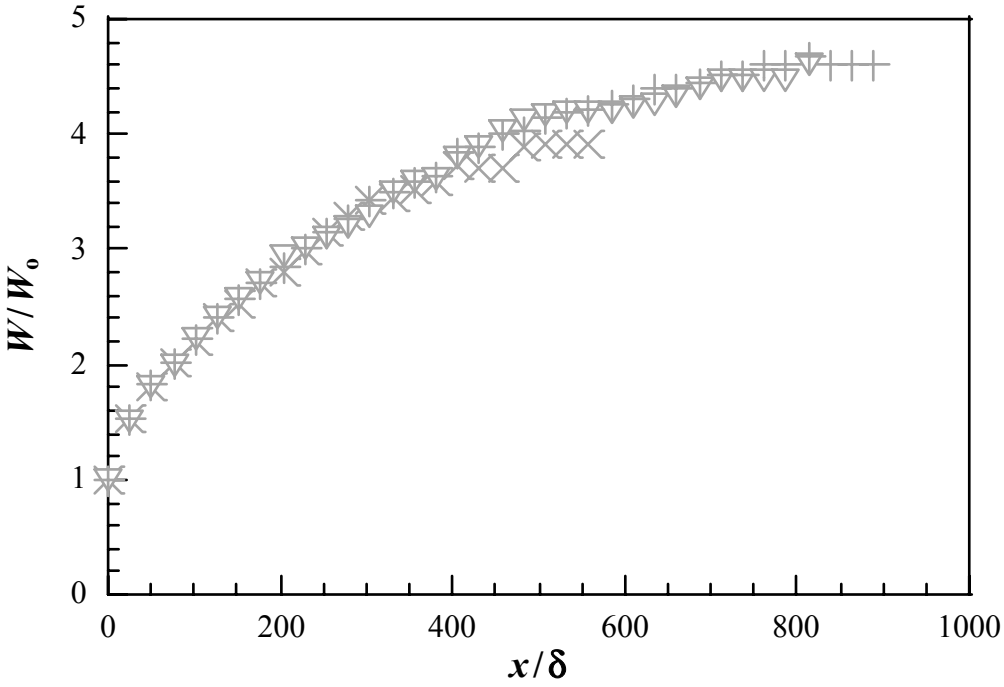

Figure 7

Anderson *et al.*

Ms-272402

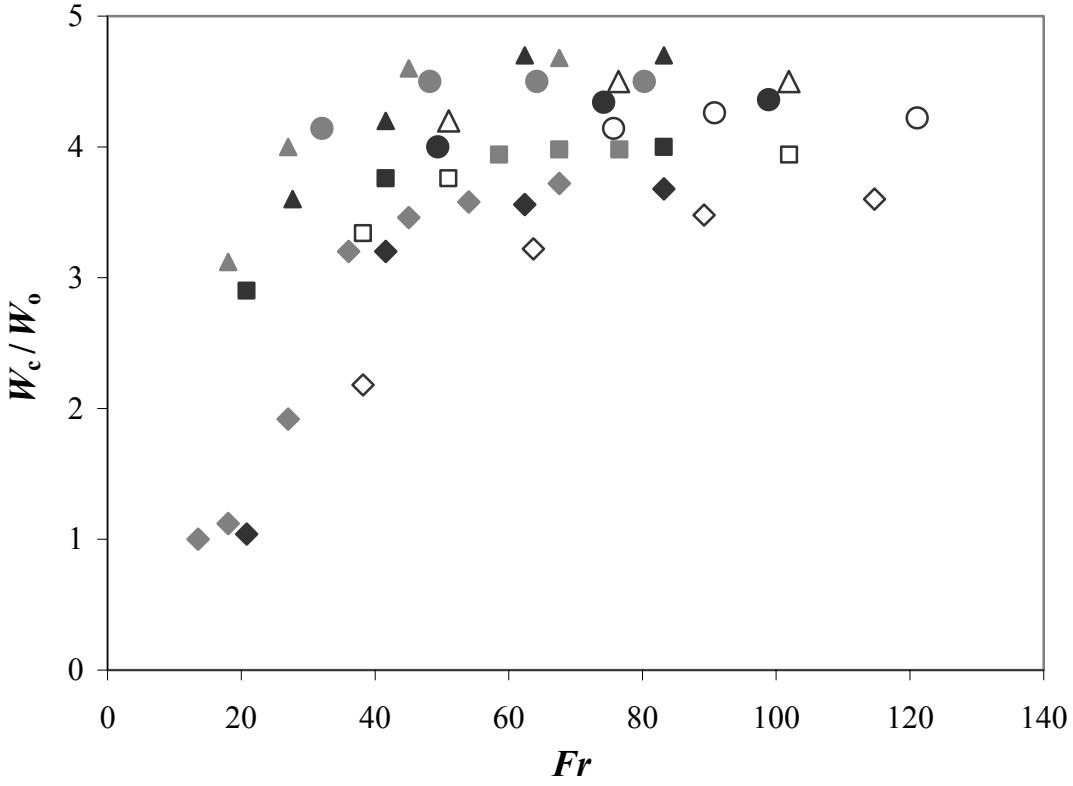

Figure 8

Anderson *et al.*

Ms-272402